recycling

MDPI

Article

Efficient Extraction of Lithium, Cobalt, and Nickel from Nickel-Manganese-Cobalt Oxide Cathodes with Cholin Chloride/Pyrogallol-Based Deep Eutectic Solvent

Aisulu Batkal [1,2], Kaster Kamunur [1,2], Lyazzat Mussapyrova [1], Yerzhan Mukanov [3] and Rashid Nadirov [1,2,*]

[1] Institute of Combustion Problems, Almaty 050012, Kazakhstan; abatkalova@mail.ru (A.B.); kamunur.k@mail.ru (K.K.); lyazzat.mussapyrova@gmail.com (L.M.)
[2] Faculty of Chemistry and Chemical Technology, Al-Farabi Kazakh National University, Almaty 050040, Kazakhstan
[3] School of Materials Science and Green Technologies, Kazakhstan-British Technical University, Almaty 050000, Kazakhstan; ymukmail@gmail.com
* Correspondence: nadirov.rashid@gmail.com; Tel.: +7-747-452-05-25

Abstract: This study explores the use of a deep eutectic solvent (DES) composed of choline chloride and pyrogallol (1:1 molar ratio) for the recovery of lithium, cobalt, and nickel from spent lithium-ion battery cathodes based on $LiNi_{0.33}Co_{0.33}Mn_{0.33}O_2$ (NMC111). The DES exhibits moderate viscosity, intrinsic redox activity, and strong complexation ability, enabling efficient metal dissolution under mild conditions. The effects of both temperature (50–80 °C) and time (up to 12 h) on leaching efficiency were systematically investigated. Optimal leaching parameters—80 °C, 8 h, and a liquid-to-solid ratio of 50—yielded extraction efficiencies of 92% for Li, 85% for Co, and 88% for Ni. Kinetic modeling indicated pseudo-first-order behavior with activation energies of 26.6, 22.1, and 25.2 kJ/mol for Li, Co, and Ni, respectively. Mechanistic analysis confirmed the dual role of pyrogallol as both reducing agent (facilitating Co^{3+} to Co^{2+} conversion) and chelating ligand.

Keywords: lithium-ion batteries (LIBs); metal leaching; deep eutectic solvents (DESs); pyrogallol; choline chloride; NMC cathode

check for updates

Academic Editor: Ana Paula Paiva

Received: 27 March 2025
Revised: 28 April 2025
Accepted: 1 May 2025
Published: 3 May 2025

Citation: Batkal, A.; Kamunur, K.; Mussapyrova, L.; Mukanov, Y.; Nadirov, R. Efficient Extraction of Lithium, Cobalt, and Nickel from Nickel-Manganese-Cobalt Oxide Cathodes with Cholin Chloride/Pyrogallol-Based Deep Eutectic Solvent. *Recycling* **2025**, *10*, 88. https://doi.org/10.3390/recycling10030088

Copyright: © 2025 by the authors. Licensee MDPI, Basel, Switzerland. This article is an open access article distributed under the terms and conditions of the Creative Commons Attribution (CC BY) license (https://creativecommons.org/licenses/by/4.0/).

1. Introduction

The widespread use of lithium-ion batteries (LIBs) in electric vehicles, renewable energy, and consumer electronics has sharply increased end-of-life LIB waste. These batteries are considered in two aspects—as environmental pollutants and as sources of valuable metals such as lithium, cobalt, and nickel [1–3]. Thus, finding efficient ways to recover these metals from spent lithium batteries is an important task.

Traditional methods for LIB recycling, such as pyrometallurgical and acid-based hydrometallurgical processes, are often energy-intensive, generate hazardous emissions, and lack selectivity toward individual metal components [4–6]. In response to these limitations, deep eutectic solvents (DESs) have emerged as a promising class of alternative leaching media. DESs are typically formed by combining a hydrogen bond acceptor (HBA)—commonly choline chloride (ChCl)—with a hydrogen bond donor (HBD) such as urea, organic acids, or polyols [7–10]. These solvents exhibit low vapor pressure, high thermal stability, and the ability to solvate a wide range of inorganic and organic species.

The application of DESs in LIB recycling has gained considerable traction over the past decade [11–14]. For instance, Abbott et al. were among the first to utilize a ChCl/urea DES for leaching Li and Co from $LiCoO_2$, achieving moderate extraction efficiency and

showcasing DESs as greener alternatives to traditional mineral acids [15]. In a separate study, Huang et al. introduced a ternary DES composed of choline chloride, succinic acid, and ethylene glycol (ChCl/SA/EG), which enabled the complete dissolution of $LiCoO_2$ at 140 °C within 16 h, with an activation energy as low as 11.77 kJ/mol [16]. Suriyanarayanan et al. developed a nonionic DES system based on N-methylurea and acetamide, capable of selectively leaching over 97% Co from $LiCoO_2$ under mild conditions; here, N-methylurea served a dual role as both a solvent and reductant, reducing Co^{3+} to Co^{2+} without external reducing agents [17]. Septioga et al. proposed an innovative DES–aqueous biphasic system using 4,4,4-trifluoro-1-phenyl-1,3-butanedione and tri-n-octylphosphine oxide, achieving 99% Li leaching from $LiCoO_2$ at 80 °C in 24 h, with lithium transferred in situ to the aqueous phase, while cobalt remained in the DES layer—facilitating downstream separation [18]. In another example, Li et al. evaluated ChCl-based DESs such as ChCl/ethylene glycol for NMC cathodes and reported a >99% extraction of Li, Co, and Ni, albeit with kinetics 2–3 orders of magnitude slower than those of inorganic acid leaching [19]. More recently, Ketegenov et al. applied ultrasound-assisted leaching in a polyethylene glycol-based DES, enhancing metal recovery and reducing the processing time; 98.2% Co and Li were extracted at 90 °C within 2 h, due to improved mass transfer and viscosity reduction induced by ultrasound [20]. Table 1 summarizes representative examples of DES-based leaching approaches, including the cathode material, DES compositions, operating conditions, and metal recovery rates.

Table 1. Leaching efficiencies of various DESs for different cathode materials.

Cathode Material	DES Composition	Temperature (°C)	Time (min)	Leaching Efficiency (%)	Ref.
NMC	Betaine hydrochloride/ethylene glycol (1:5)	140	10	>99% for Co, Ni, Mn, Li	[21]
LCO	Choline chloride/levulinic acid (1:4)	80	10	>90% for Co, Li	[22]
NMC	Choline chloride/ethylene glycol (1:2)	80	30	98.8% Co, 99.1% Ni, 99.2% Mn, 99.8% Li	[23]
NMC	Choline chloride/ethylene glycol (1:2)	80	60	99% for Co, Ni, Mn, Li	[24]
LCO	Choline chloride/citric acid (1:2)	90	120	95% for Co, Li	[21]
LCO	Choline chloride/oxalic acid (1:1)	85	60	92% for Co, Li	[25]
NMC	Choline chloride/urea (1:2)	100	120	96% for Co, Ni, Mn, Li	[26]

Among the growing array of DES systems, particular attention has recently been given to those incorporating redox-active HBDs, especially phenolic compounds. Pyrogallol (1,2,3-trihydroxybenzene) is one such HBD capable of not only forming stable eutectic mixtures with choline chloride but also participating in electron transfer reactions [27–29]. Previous studies have shown that DESs based on ChCl and pyrogallol exhibit moderate viscosity and high conductivity, as well as intrinsic reducing power due to the ease of oxidation of pyrogallol to o-quinone derivatives. A DES synthesized from ChCl and pyrogallol in a 1:2 molar ratio exhibits moderate viscosity (~300–500 cP at 25 °C) and increased ionic conductivity (3–5 mS/cm) compared to other phenolic HBD-based DESs, and is stable up to 150 °C, making it suitable for leaching processes at moderate temperatures (80–120 °C) [27]. Pyrogallol in a DES is easily oxidized to ortho-quinone derivatives by radicals (e.g., peroxyl) or electrochemically, as confirmed by spectroelectrochemical studies [30].

Despite the existing body of work on ChCl/pyrogallol DES, its application for the selective leaching of critical metals from layered oxide cathode materials remains poorly explored; only a single study has specifically addressed its use for leaching LIB cathodes [25].

While the ChCl/pyrogallol system has been previously characterized with respect to its antioxidant, electrochemical, and solvation properties, its use in hydrometallurgical metal recovery has not been systematically explored. In particular, the potential of this system to promote the reductive dissolution of Co(III), in parallel with the proton-assisted leaching of Li and ligand complexation of Ni(II), presents an attractive pathway for integrated recovery.

While various DES-based systems have been explored for lithium-ion battery recycling, most studies have focused on simple hydrogen bond, often requiring additional reducing agents to facilitate cobalt dissolution. In contrast, the ChCl/pyrogallol system investigated in this work integrates reductive and complexation functionalities within a single solvent phase, enabling Co^{3+} reduction and metal solubilization without external reductants.

In this study, we examine the application of a ChCl/pyrogallol DES (1:1 molar ratio) for the recovery of lithium, cobalt, and nickel from a $LiNi_{0.33}Co_{0.33}Mn_{0.33}O_2$ cathode material sourced from spent LIBs. The leaching behavior of Li, Co, and Ni in this medium was evaluated under various operational parameters, including temperature, leaching duration, and liquid-to-solid ratio. Kinetic modeling and activation energy calculations were performed to elucidate the dissolution mechanisms. In addition, the specific role of pyrogallol as both a redox-active component and coordinating ligand is discussed in the context of selective metal extraction from complex oxide matrices.

2. Materials and Methods

2.1. Materials

The cathode material was manually separated from spent lithium-ion batteries. Prior to disassembly, spent lithium-ion batteries were immersed in a 5 wt% sodium chloride solution for 48 h to safely discharge residual energy. After drying, the cells were manually opened, and the cathode layers were mechanically separated from the aluminum current collectors using a plastic spatula. The recovered cathode powder was thoroughly washed with ethanol and distilled water to remove electrolyte residues and binder components, followed by drying at 60 °C for 12 h. Approximately 5 g of cathode material was manually recovered and used for the leaching experiments and analytical characterization described in this work.

Choline chloride (≥99%) and pyrogallol (≥99%) were purchased from Sigma-Aldrich and used without further purification.

2.2. Synthesis of Deep Eutectic Solvent

The DES was prepared by mixing choline chloride and pyrogallol in a 1:1 molar ratio. The mixture was heated at 95 °C under continuous stirring until a homogeneous and transparent liquid was obtained. The total amount of the DES synthesized for this study was approximately 400 g, prepared in laboratory batches of 20 to 50 g depending on the experimental series. The prepared DES was stored in a desiccator prior to use.

2.3. Leaching Experiments

Leaching tests were carried out in glass reactors with reflux under constant magnetic stirring. In each test, 0.1 g of cathode powder was added to a pre-determined amount of the DES. The leaching temperature was maintained at 50, 70, 80, or 100 °C using a thermostatic oil bath. Samples were collected at regular time intervals (1 h).

2.4. Analysis of Metal Content

The chemical composition of both the leachate and the cathode material was determined by atomic absorption spectrometry (AAS) using a GBC Savant spectrometer (GBC Scientific Equipment Pty Ltd., Keysborough, Australia). For solid samples, complete microwave-assisted acid digestion in a HCl/H_2O_2 mixture at 80 °C for 2 h was performed prior to analysis. Calibration was carried out using certified standard solutions, and the measurement accuracy was within ±2%. All measurements were performed in triplicate, with relative standard deviations (RSDs) not exceeding ±3%. The extraction efficiency was calculated as the ratio of the amount of metal leached into the solution to its total content in the initial solid sample. The results were expressed as a percentage of the extracted amount relative to the original metal content.

2.5. X-Ray Diffraction Analysis

An X-ray diffraction (XRD) analysis of the cathode material was performed using Cu-Kα radiation (λ = 1.5406 Å) in the 2θ range of 10–80°, with a step size of 0.02° and a scan rate of 2°/min, using a D8 Advance diffractometer (Bruker)

2.6. UV–Vis Spectroscopy

UV-Vis absorption spectra were recorded using a CF-56 (Russia) spectrophotometer in the range of 200–800 nm using quartz cuvettes.

2.7. Fourier-Transform Infrared (FTIR) Spectroscopy

Fourier-transform infrared (FTIR) spectroscopy was carried out in the range of 4000–400 cm^{-1} with a resolution of 4 cm^{-1} using an Infralum FT-08 spectrometer (NPF Lumex, Russia). For the FTIR analysis of solid samples, the leached cathode powder was washed with ethanol to remove residual DES, dried at 60 °C for 12 h, mixed with KBr, and pressed into pellets. For the DES liquid samples, thin films were prepared by placing a drop of the DES between two KBr plates.

2.8. Physicochemical Characterization of the DES

The viscosity of the ChCl/pyrogallol DES was measured at 80 °C using a VPZh-4M capillary viscometer (Russia) in accordance with GOST 33-2000.

Electrical conductivity was determined using an AKP-01 “EconTest” conductometer (Russia) equipped with a platinum conductivity cell (κ = 1.0 cm^{-1}).

To assess the relative acidity of the solvent, a 10 wt% aqueous dilution of the DES was prepared with distilled water. The pH of the solution was measured using a pH-150MI pH meter (Izmeritel, Russia) with a combined glass electrode (ESK-10601).

3. Results and Discussion

3.1. Characterization of the Cathode Material

The XRD pattern of the sample is presented in Figure 1. It reveals characteristic peaks corresponding to the hexagonal crystal structure, typical of layered lithium nickel–cobalt–manganese oxide at 18.7°, 36.5°, 44.6°, 58.3°, and 69.2°, that correspond to the $LiNi_xCo_\gamma Mn_xO_2$ phase. The most intense peak at approximately 26.5° 2θ is attributed to the (002) plane of graphite.

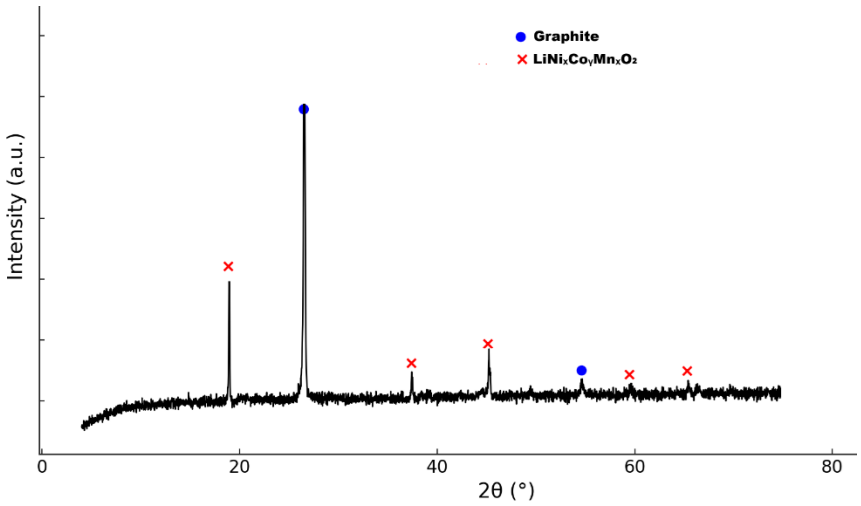


Figure 1. The XRD pattern of the cathode material matching the layered $LiNi_xCo_YMn_xO_2$ structure (PDF 01-089-3084).

The chemical composition of the cathode material is presented in Table 2.

Table 2. The chemical composition of the cathode.

Li (wt %)	Co (wt %)	Ni (wt %)	Mn (wt %)
6.81	19.07	18.94	17.72

The thermal treatment of the cathode powder at 650 °C for 3 h resulted in a mass loss of approximately 6%, indicating the removal of organic binders and conductive carbon additives. After this treatment, the remaining solid residue is consistent with the stoichiometry of the active phase $LiNi_{0.33}Co_{0.33}Mn_{0.33}O_2$, confirming that the sample predominantly contains the layered oxide component used in NMC-type cathodes.

An SEM image of the cathode material powder (Figure 2) shows irregularly shaped secondary particles with sizes ranging from approximately 1 to 15 µm, consistent with the morphology typically observed for NMC-type layered oxide powders manually separated from aluminum current collectors. The particle structure suggests the partial fragmentation of the cathode layer during mechanical separation, which is typical for materials recovered from spent lithium-ion batteries.

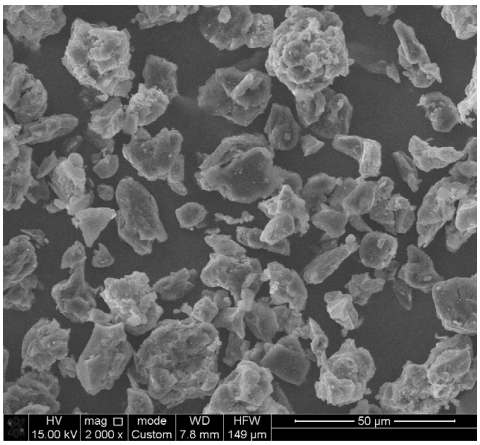


Figure 2. An SEM image of the recovered NMC cathode material.

3.2. DES Characterization

The DES composed of choline chloride and pyrogallol in a 1:1 molar ratio formed a homogeneous, viscous brown liquid when heated to 80 °C under constant stirring. The DES remained stable in the temperature range of 30–90 °C during leaching experiments, with no visible phase separation or precipitation observed over 24 h.

FTIR spectroscopy was used to confirm the formation of hydrogen bonding interactions between choline chloride and pyrogallol (Figure 3). In the DES spectrum, the broad O–H stretching band (3200–3500 cm^{-1}) was significantly broadened and shifted compared to the spectra of the individual components, indicating extensive hydrogen bonding. The C–O and aromatic C=C stretching vibrations also showed minor shifts, suggesting an interaction between the phenolic groups of pyrogallol and the chloride ion of choline chloride. The apparent suppression of C–H bending and C–N stretching vibrations in the DES spectrum can be explained by strong hydrogen bonding between choline chloride and pyrogallol. Such interactions cause a significant broadening and overlap of vibrational bands, particularly in the O–H stretching and bending regions, which may mask or redistribute the C–H and C–N signals.

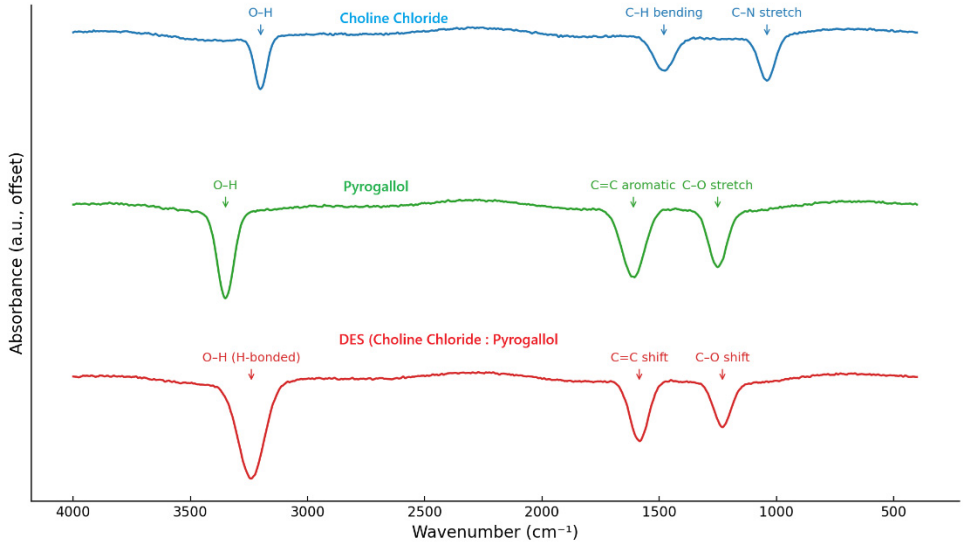


Figure 3. FTIR spectra of choline chloride, pyrogallol, and their deep eutectic mixture (ChCl/pyrogallol, 1:1 mol/mol).

The physicochemical properties of the DES are summarized in Table 3.

Table 3. Physicochemical properties of choline chloride, pyrogallol, and their deep eutectic solvent (ChCl/pyrogallol, 1:1 mol/mol).

System	pH (10% aq.)	Viscosity at 80 °C (mPa·s)	Conductivity at 25 °C (mS/cm)	Appearance
Choline Chloride	6.8	-	-	White powder
Pyrogallol	4.1	-	-	Brown crystals
DES (ChCl/Pyrogallol, 1:1)	4.3	19	3.2	Homogeneous brown liquid

The DES based on choline chloride and pyrogallol exhibited a viscosity of 19 mPa·s at 80 °C, which is lower than that of the conventional ChCl/urea DES (~90–100 mPa·s at the same temperature). The DES exhibited a moderately acidic pH (measured as a 10% aqueous solution) of approximately 4.3, which can promote metal dissolution. The moderate viscosity of the system may enhance mass transfer and metal dissolution kinetics

during leaching. The electrical conductivity of the DES was also relatively high (3.2 mS/cm at 25 °C), likely due to the presence of ionic and π-conjugated species.

3.3. Leaching Behavior

Figure 4 shows the UV-Vis spectra of DES after contact with the cathode material (0.1 g/5 g) at 90 °C after a certain period of time (15, 30, 60, 120 and 240 min).

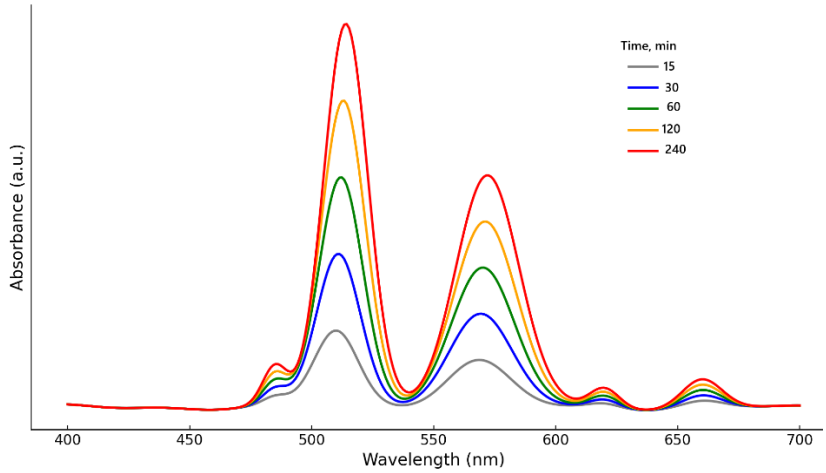


Figure 4. UV-Vis absorption spectra of the leachate obtained after different leaching times using ChCl/pyrogallol DES.

All spectra show two dominant peaks with maxima in the range of 510–515 nm and 568–573 nm, corresponding to d–d transitions in Co^{2+} ions complexed with the phenolic groups of pyrogallol. The increase in the intensity of these bands with increasing time indicates a progressive reduction of Co^{3+} to Co^{2+} and subsequent stabilization in the solution in the form of phenolate complexes. Additionally, weak absorption bands were recorded in the region of 485 nm (a possible contribution of Ni^{2+}), as well as in the region of 620 and 660 nm, which may be associated with the formation of weak Mn^{2+} complexes and/or colloidal particles. The background line of the spectra has a characteristic wavy shape, which is due to internal electron transitions in pyrogallol and its interaction with metal centers. Shifts in absorption maxima by 2–3 nm with increasing time may indicate a gradual restructuring of the coordination environment, for example, from monodentate to chelate structures.

To justify the possibility of reducing cobalt(III) to cobalt(II) under the conditions of the proposed system, a simplified Pourbaix diagram for cobalt was constructed (Figure 5). While not directly applicable to DES, it provides a useful conceptual framework suggesting that Co^{3+} may be reduced to Co^{2+} by pyrogallol under moderately acidic conditions (pH~4.3, E ≈ +0.5 V).

The diagram allows one to estimate the thermodynamic stability of various forms of cobalt depending on the pH of the medium and the oxidation–reduction potential. Considering that the ChCl/pyrogallol-based medium has a pH of ≈4.3, and pyrogallol has a reduction potential of about +0.5 V (vs NHE), the working point of the system is plotted on the diagram as a black cross. As can be seen, it falls within the stability region of soluble Co^{2+}. This confirms that the reduction of Co^{3+} and its transition to solution in the form of complexes with pyrogallol is possible without adding external reducing agents, which is consistent with the observed results of the UV spectroscopy.

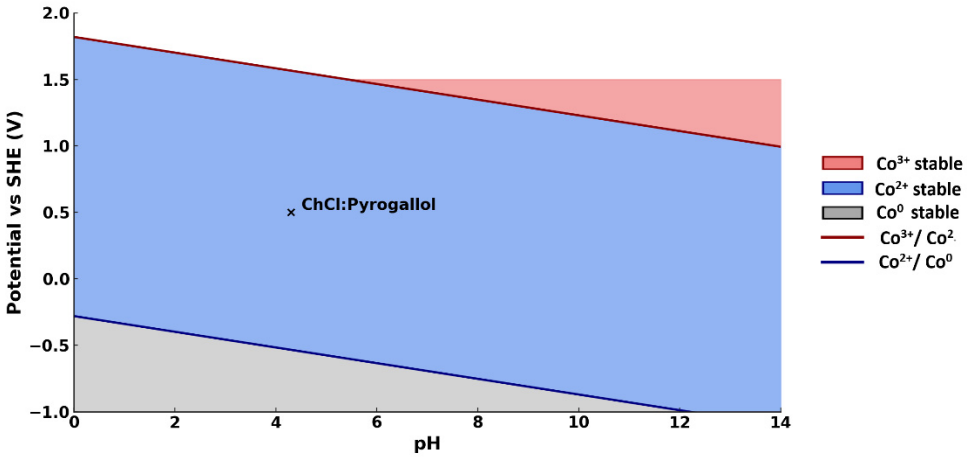


Figure 5. A Pourbaix diagram for cobalt with the working point of ChCl/pyrogallol DES (pH ≈ 4.3, E ≈ +0.5 V) marked by a black cross.

The next series of experiments was devoted to the study of the quantitative extraction of Li, Co and Ni into solution. Due to the low economic value of Mn and its low leaching efficiency under the studied conditions, manganese was not considered a priority element in the scope of this work.

Figure 6 shows the extraction efficiency of Li, Co, and Ni from the cathode material into the DES at 80 °C and a liquid-to-solid ratio of 50 (0.1 g solid per 5 g DES).

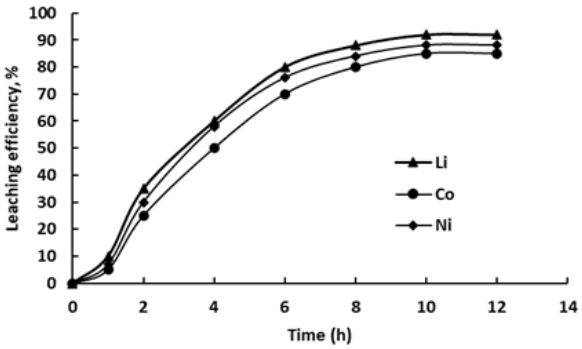


Figure 6. Dependence of Li, Co and Ni recovery into ChCl/pyrogallol-based DES on leaching duration (L:S = 10 g/g, 80 °C).

All three metals show rapid extraction in the first 4–6 h. Li leaching is the fastest, reaching 60% after 4 h and 80% by 6 h. Co and Ni follow a similar trend, with Co reaching 50% and Ni 58% at 4 h. Between 6 and 8 h, the extraction rate slows down, approaching a plateau: at 8 h, Li reaches 88%, Co 80%, and Ni 84%. Further leaching up to 12 h results in only minor improvements, with maximum extraction values of 92% for Li, 85% for Co, and 88% for Ni.

Figure 7 illustrates the effect of the liquid-to-solid ratio on the extraction efficiency of the mentioned metals into the DES at 80 °C after 8 h of leaching.

An increase in the L:S ratio from 30 to 50 g/g significantly enhances metal recovery, with extraction improving from 70% to 92% for Li, from 55% to 85% for Co, and from 58% to 88% for Ni. Further increases beyond L:S = 50 yield only marginal improvements, with all three metals reaching a plateau. These results indicate that an L:S ratio of 50 is optimal for efficient metal extraction under the studied conditions.

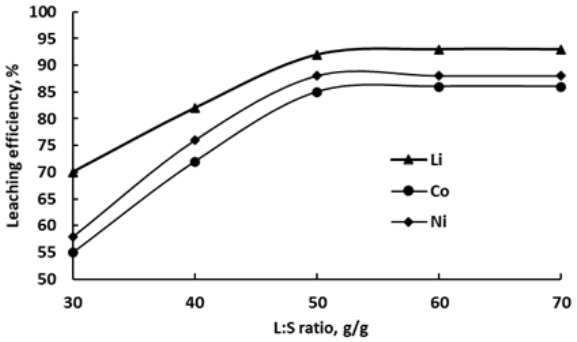


Figure 7. Dependence of Li, Co and Ni recovery into ChCl/pyrogallol-based DES on L:S ratio (8 h, 80 °C).

Figure 8 demonstrates the temperature-dependent extraction behavior of the studied metals into the DES under constant leaching conditions (8 h, L:S ratio = 50). A marked enhancement in extraction efficiency is observed with increasing temperature in the range of 50–80 °C. Specifically, Li recovery improves from 65% to 92%, Co from 40% to 85%, and Ni from 45% to 88%. A further temperature increase to 100 °C yields only negligible improvement, indicating that 80 °C represents the optimal balance between extraction performance and energy input.

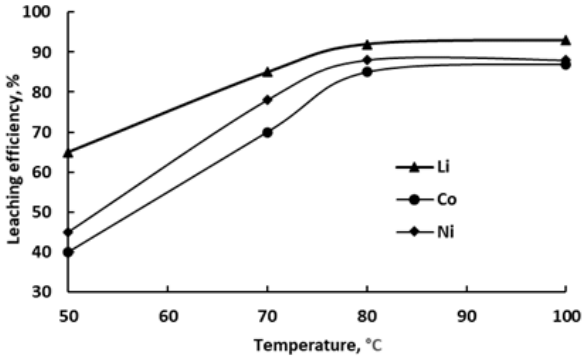


Figure 8. Dependence of Li, Co and Ni recovery into ChCl/pyrogallol-based DES on temperature (8 h, L:S = 50).

Thus, the following optimal leaching conditions were identified for the ChCl/pyrogallol (1:1 mol) system applied to the $LiNi_{0.33}Co_{0.33}Mn_{0.33}O_2$ (NMC111) cathode material: a temperature of 80 °C, a leaching duration of 8 h, and a liquid-to-solid ratio of 50 (g/g). Under these parameters, maximum extraction efficiencies of 92% for Li, 85% for Co, and 88% for Ni were achieved.

3.4. Leaching Kinetic Analysis

To better understand the dissolution behavior of Li, Co, and Ni from the NMC cathode in the ChCl/pyrogallol (1:1 mol.) DES, a kinetic study was performed under varying temperatures. The leaching process was evaluated assuming a pseudo-first-order reaction model, which is commonly applied to solid–liquid leaching systems [31,32]. The degree of metal extraction was monitored over time at 50, 70, and 80 °C, and the leaching kinetics of Li, Co, and Ni were evaluated using the pseudo-first-order model. The model assumes that the rate of dissolution is proportional to the concentration of the unreacted solid phase. The differential rate law can be written as follows:

$$\frac{d(1-X)}{dt} = -k(1-X)$$

where X is the fraction of metal extracted into the solution, k is the apparent rate constant (h^{-1}), and t is the leaching time.

The integration of this equation yields the following linearized form:

$$\ln(1 - X) = -kt$$

By plotting $\ln(1 - X)$ versus t, a straight line is obtained, and the slope of this line corresponds to the rate constant kk. This method was applied to the leaching data at 50, 70, and 80 °C for each metal. The calculated kk values were then used in the Arrhenius equation to determine the activation energies.

The corresponding dependencies are shown in Figure 9a–c.

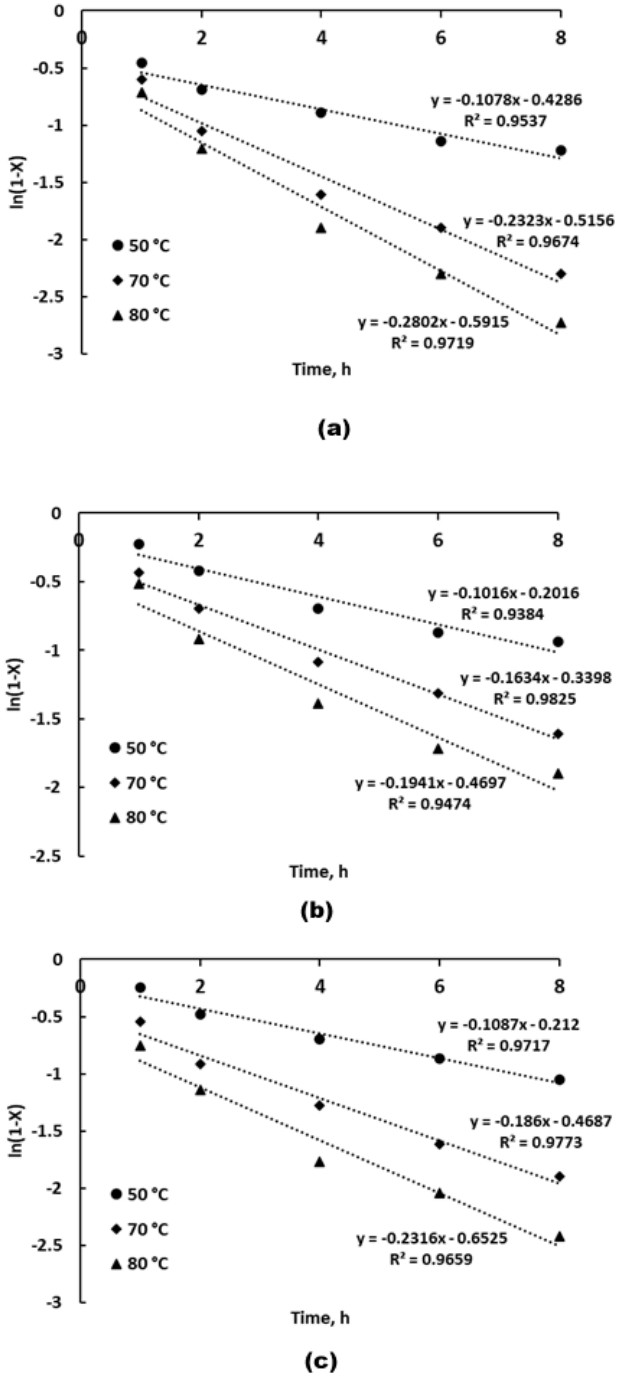


Figure 9. Plots of ln(1−X) vs. leaching time for Li (**a**), Co (**b**), and Ni (**c**) into ChCl/pyrogallol-based DES at different temperatures.

The values of the apparent rate constants for metal leaching at different temperatures, as well as the determination coefficients (R^2) of the corresponding linear regressions based on the pseudo-first-order model, are summarized in Table 4.

Table 4. Apparent rate constants and determination coefficients for Li, Co, and Ni leaching from NMC cathode in ChCl/pyrogallol DES (pseudo-first-order model).

Temperature (°C)	Metal	k, h^{-1}	R^2
50	Li	0.108	0.954
	Co	0.102	0.938
	Ni	0.109	0.972
70	Li	0.232	0.967
	Co	0.163	0.983
	Ni	0.186	0.977
80	Li	0.280	0.972
	Co	0.194	0.947
	Ni	0.232	0.966

Among the three metals, Li exhibits the highest rate constants at all temperatures, reaching 0.302 h^{-1} at 80 °C, followed by Ni and Co. This trend suggests that Li is the most readily leached element, likely due to its position in the layered oxide structure and its high mobility. Cobalt shows the lowest leaching rates, which may be attributed to its initial oxidation state (Co^{3+}) and the need for reduction prior to dissolution. The high R^2 values (0.938–0.983) for all regressions confirm the applicability of the pseudo-first-order model to describe the leaching kinetics of all three metals under the studied conditions.

To visualize the temperature dependence of the leaching rate, an Arrhenius plot was constructed by plotting ln k against the reciprocal of absolute temperature (Figure 10).

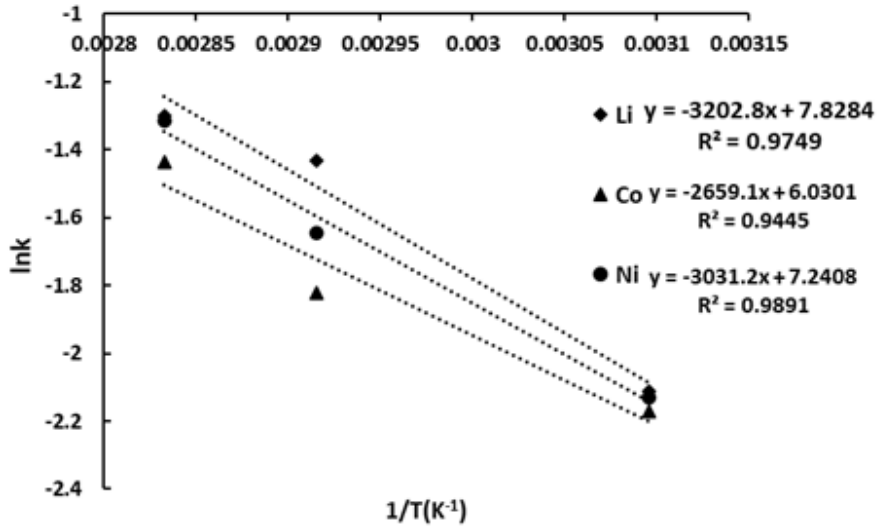


Figure 10. Arrhenius plot for Li, Co and Ni recovery into ChCl/pyrogallol-based DES (L:S = 50 g/g).

The calculated activation energies (E_a) of the reactions of extraction of Li, Co and Ni into solution were, respectively, in kJ/mol, 26.62, 22.11, and 25.20. These values are within the typical range for diffusion- and surface-reaction-controlled processes, suggesting a mixed kinetic regime under the applied conditions [33].

The slightly lower Ea observed for cobalt may be attributed to the redox-active nature of the solvent system. Pyrogallol, as an electron-donating ligand, likely facilitates the reduction of Co^{3+} to the more soluble Co^{2+} state, effectively lowering the energy barrier for its dissolution. In contrast, the extraction of lithium and nickel proceeds without redox conversion, relying primarily on proton exchange and ligand solvation, which could account for their relatively higher activation energies. Furthermore, the comparable Ea values for Li and Ni indicate similar sensitivity to temperature, possibly reflecting their parallel behavior within the layered oxide matrix of the NMC cathode.

3.5. Mechanistic Considerations

The leaching mechanism of Li, Co, and Ni from the layered $LiNi_{0.33}Co_{0.33}Mn_{0.33}O_2$ (NMC111) cathode in ChCl/pyrogallol DES involves a combination of redox transformation, proton-assisted lattice disruption, and ligand complexation. The kinetic data obtained under various temperatures confirmed pseudo-first-order behavior, with apparent activation energies of 26.6 kJ/mol for Li, 22.1 kJ/mol for Co, and 25.2 kJ/mol for Ni, indicating moderate energy barriers consistent with surface-controlled dissolution and complexation processes.

In the crystal structure of NMC111, Co, Ni, and Mn occupy octahedral sites within the MO_6 layers, while Li resides in interlayer positions [34]. Cobalt exists predominantly as Co^{3+}, requiring reduction to Co^{2+} prior to dissolution. Pyrogallol, a redox-active phenolic ligand, serves as an intrinsic electron donor in the DES, reducing Co^{3+} via a ligand-to-metal charge transfer mechanism:

$$2Co^{3+}{}_{(s)} + C_6H_3(OH)_3 = 2Co^{2+}{}_{(l)} + C_6H_3(OH)_3{}^{2+}$$

The reduced Co^{2+} is stabilized in the solution via coordination with hydroxyl and carbonyl groups of the oxidized pyrogallol species. This reaction proceeds with the lowest activation energy among the three metals, consistent with the facilitated electron transfer pathway and the strong complexation environment provided by the DES.

The dissolution of cobalt also plays a structural role: the extraction of Co from the MO_6 layers leads to the destabilization of the layered oxide lattice, increasing defect density and enhancing the accessibility of the remaining metal cations to the solvent phase. As a result, the extraction of Li^+ and Ni^{2+} is promoted once cobalt begins to leach. This is further supported by the similar activation energies and nearly parallel kinetic profiles of Li and Ni, suggesting that their leaching becomes increasingly favorable as the structure degrades. This behavior is consistent with literature reports showing that the extraction of cobalt from MO_6 layers destabilizes the layered oxide structure and promotes the increased mobility of lithium and nickel ions due to lattice distortion and defect formation [35].

Li extraction occurs via ion exchange with labile protons in the solvent network, disrupting the interlayer structure and releasing Li^+ into the liquid phase:

$$LiMO_{2(s)} + H^+ = HMO_{2(s)} + Li^+{}_{(l)}$$

Nickel, present as Ni^{2+} in the NMC lattice, does not require redox transformation for dissolution. However, its extraction is facilitated by complexation with donor ligands available in the DES. In this system, pyrogallol can undergo a partial deprotonation of its phenolic –OH groups, especially in the coordination environment around metal centers. The resulting phenolate anions (Pg^-), stabilized through hydrogen bonding within the DES matrix, serve as bidentate or multidentate ligands, forming stable complexes with Ni^{2+}:

$$Ni^{2+}_{(s)} + 2\,Pg^{-} = [Ni(Pg)_2]_{(l)}$$

Here, Pg^{-} represents the monoanionic form of pyrogallol formed by the loss of one proton from each phenolic hydroxyl group. Such deprotonated ligands enhance the solubility of Ni^{2+} by stabilizing it in the liquid phase through chelation. The presence of chloride ions in the DES may also contribute to mixed-ligand complex formation, further facilitating Ni release from the solid phase.

The observed increase in rate constants with temperature, together with the moderate activation energies, suggests a leaching mechanism limited by surface complexation and solid-state diffusion rather than transport through the bulk DES.

4. Conclusions

In this work, a DES based on choline chloride and pyrogallol (1:1 mol/mol) was evaluated for the leaching of Li, Co, and Ni from spent lithium-ion battery NMC111 cathode material.

The system demonstrated high leaching efficiency under mild conditions, achieving extraction values of 92% for Li, 85% for Co, and 88% for Ni at 80 °C within 8 h. Kinetic modeling confirmed pseudo-first-order behavior, with moderate activation energies (26.6 kJ/mol for Li, 22.1 kJ/mol for Co, and 25.2 kJ/mol for Ni), suggesting surface-controlled dissolution.

Mechanistic analysis indicated that pyrogallol plays a dual role: it acts as a mild reducing agent, enabling the conversion of Co^{3+} to Co^{2+}, and as a coordinating ligand for transition metals. The dissolution of Co promotes lattice destabilization, facilitating the subsequent extraction of Li and Ni.

Author Contributions: Conceptualization, R.N. and K.K.; methodology, A.B., K.K. and L.M.; investigation, Y.M., L.M. and A.B.; resources, R.N.; writing—original draft preparation, K.K., Y.M. and A.B.; writing—review and editing, R.N. and L.M.; project administration, R.N. All authors have read and agreed to the published version of the manuscript.

Funding: This research was funded by the Science Committee of the Ministry of Science and Higher Education of the Republic of Kazakhstan (Grant No. AP19679106).

Data Availability Statement: The data supporting the results can be made available from the corresponding author upon request.

Conflicts of Interest: The authors declare no conflicts of interest.

References

1. Zhang, N.; Xu, Z.; Deng, W.; Wang, X. Recycling and upcycling spent LIB cathodes: A comprehensive review. *Electrochem. Energy Rev.* **2022**, *5* (Suppl. 1), 33. [CrossRef]
2. Li, L.; Zhang, X.; Li, M.; Chen, R.; Wu, F.; Amine, K.; Lu, J. The recycling of spent lithium-ion batteries: A review of current processes and technologies. *Electrochem. Energy Rev.* **2018**, *1*, 461–482. [CrossRef]
3. Wei, Q.; Wu, Y.; Li, S.; Chen, R.; Ding, J.; Zhang, C. Spent lithium ion battery (LIB) recycle from electric vehicles: A mini-review. *Sci. Total Environ.* **2023**, *866*, 161380. [CrossRef] [PubMed]
4. Cornelio, A.; Zanoletti, A.; Bontempi, E. Recent progress in pyrometallurgy for the recovery of spent lithium-ion batteries: A review of state-of-the-art developments. *Curr. Opin. Green Sustain. Chem.* **2024**, *46*, 100881. [CrossRef]
5. Asadi Dalini, E.; Karimi, G.; Zandevakili, S.; Goodarzi, M. A review on environmental, economic and hydrometallurgical processes of recycling spent lithium-ion batteries. *Miner. Process. Extr. Metall. Rev.* **2021**, *42*, 451–472. [CrossRef]
6. Chagnes, A.; Pospiech, B. A brief review on hydrometallurgical technologies for recycling spent lithium-ion batteries. *J. Chem. Technol. Biotechnol.* **2013**, *88*, 1191–1199. [CrossRef]
7. Zante, G.; Boltoeva, M. Review on hydrometallurgical recovery of metals with deep eutectic solvents. *Sustain. Chem.* **2020**, *1*, 238–255. [CrossRef]

8. Guo, M.; Deng, R.; Gao, M.; Xu, C.; Zhang, Q. Sustainable recovery of metals from e-waste using deep eutectic solvents: Advances, challenges, and perspectives. *Curr. Opin. Green Sustain. Chem.* **2024**, *47*, 100913. [CrossRef]
9. Tian, G.; Liu, H. Review on the mineral processing in ionic liquids and deep eutectic solvents. *Miner. Process. Extr. Metall. Rev.* **2024**, *45*, 130–153. [CrossRef]
10. Topçu, M.A.; Rüşen, A.; Küçük, Ö.Z.K.A.N. Treatment of copper converter slag with deep eutectic solvent as green chemical. *Waste Manag.* **2021**, *132*, 64–73. [CrossRef]
11. Wang, Z.; Li, S.; Li, T.; Hu, T.; Ge, X. Deep eutectic solvents (DESs) for green recycling of wasted lithium-ion batteries (LIBs): Progress on pushing the overall efficiency. *Min. Metall. Explor.* **2022**, *39*, 2149–2165. [CrossRef]
12. Zhu, A.; Bian, X.; Han, W.; Cao, D.; Wen, Y.; Zhu, K.; Wang, S. The application of deep eutectic solvents in lithium-ion battery recycling: A comprehensive review. *Resour. Conserv. Recycl.* **2023**, *188*, 106690. [CrossRef]
13. Gao, W.H.; Nie, C.C.; Li, L.; Yan, S.; Zhou, W.T.; Zhu, X.N. Sustainable and efficient deep eutectic solvents in recycling of spent lithium-ion batteries: Recent advances and perspectives. *J. Clean. Prod.* **2024**, *464*, 142735. [CrossRef]
14. Wang, J.; Lyu, Y.; Zeng, R.; Zhang, S.; Davey, K.; Mao, J.; Guo, Z. Green recycling of spent Li-ion battery cathodes via deep-eutectic solvents. *Energy Environ. Sci.* **2024**, *17*, 867–884. [CrossRef]
15. Abbott, A.P.; Frisch, G.; Hartley, J.; Ryder, K.S. Processing of metals and metal oxides using ionic liquids. *Green Chem.* **2011**, *13*, 471–481. [CrossRef]
16. Huang, F.; Li, T.; Yan, X.; Xiong, Y.; Zhang, X.; Lu, S.; An, N.; Huang, W.; Guo, Q.; Ge, X. Ternary deep eutectic solvent (DES) with a regulated rate-determining step for efficient recycling of lithium cobalt oxide. *ACS Omega* **2022**, *7*, 11452–11459. [CrossRef]
17. Suriyanarayanan, S.; Babu, M.P.; Murugan, R.; Muthuraj, D.; Ramanujam, K.; Nicholls, I.A. Highly efficient recovery and recycling of cobalt from spent lithium-ion batteries using an N-Methylurea–Acetamide nonionic deep eutectic solvent. *ACS Omega* **2023**, *8*, 6959–6967. [CrossRef] [PubMed]
18. Septioga, K.; Fajar, A.T.; Wakabayashi, R.; Goto, M. Deep Eutectic Solvent-Aqueous Two-Phase Leaching System for Direct Separation of Lithium and Critical Metals. *ACS Sustain. Resour. Manag.* **2024**, *1*, 2482–2491. [CrossRef]
19. Li, B.; Li, Q.; Wang, Q.; Yan, X.; Shi, M.; Wu, C. Deep eutectic solvent for spent lithium-ion battery recycling: Comparison with inorganic acid leaching. *Phys. Chem. Chem. Phys.* **2022**, *24*, 19029–19051. [CrossRef]
20. Ketegenov, T.; Kamunur, K.; Mussapyrova, L.; Batkal, A.; Nadirov, R. Enhanced Recovery of Lithium and Cobalt from Spent Lithium-Ion Batteries Using Ultrasound-Assisted Deep Eutectic Solvent Leaching. *Metals* **2024**, *14*, 1052. [CrossRef]
21. Xu, B.; Díez, N.; Sevilla, M.; Ferrer, M.L.; Gutiérrez, M.C.; Del Monte, F. Recycling and Reutilization of Metals Aided by Deep Eutectic Solvents: From NMC Cathodes of Spent Li-ion Batteries to Electrolytes for Supercapacitors. *ChemSusChem* **2025**, *18*, e202401128. [CrossRef]
22. Bhattacharyya, S.; Roy, S.; Vajtai, R. Emerging processes for sustainable Li-ion battery cathode recycling. *Small* **2024**, 2400557. [CrossRef] [PubMed]
23. Peeters, N.; Binnemans, K.; Riaño, S. Solvometallurgical recovery of cobalt from lithium-ion battery cathode materials using deep-eutectic solvents. *Green Chem.* **2020**, *22*, 4210–4221. [CrossRef]
24. Li, Y.; Sun, M.; Cao, Y.; Yu, K.; Fan, Z.; Cao, Y. Designing Low Toxic Deep Eutectic Solvents for the Green Recycle of Lithium-Ion Batteries Cathodes. *ChemSusChem* **2024**, *17*, e202301953. [CrossRef] [PubMed]
25. Sarma, S.; Sahu, T.K.; Sharma, R.K.; Prasun, A.; Vishwakarma, R.; Kumar Sarma, T. Polyphenol Derived Natural Deep Eutectic Solvents for High Efficiency Cathode Recycling of Li-Ion Batteries. *ACS Sustain. Resour. Manag.* **2024**, *2*, 190–200. [CrossRef]
26. Qiao, W.; Zhang, R.; Wen, Y.; Wang, X.; Wang, Z.; Tang, G.; Liu, M.; Kang, H.; Said, Z.; Hwang, J.Y.; et al. Green Solvents in Battery Recycle: Status and Challenges. *J. Mater. Chem. A* **2024**, *12*, 11235–11265. [CrossRef]
27. Omar, K.A.; Sadeghi, R. Novel deep eutectic solvents based on pyrogallol: Synthesis and characterizations. *J. Chem. Eng. Data* **2021**, *66*, 2088–2095. [CrossRef]
28. Cichowska-Kopczyńska, I.; Nowosielski, B.; Warmińska, D. Deep eutectic solvents: Properties and applications in CO_2 separation. *Molecules* **2023**, *28*, 5293. [CrossRef]
29. Jaffur, B.N.; Kumar, G.; Khadoo-Jeetah, P. Enhancing deep eutectic solvent systems for efficient fermentable sugar recovery from lignocellulosic fiber. *Int. J. Biol. Macromol.* **2024**, *269*, 131888. [CrossRef]
30. Atala, E.; Velásquez, G.; Vergara, C.; Mardones, C.; Reyes, J.; Tapia, R.A.; Quina, F.; Mendes, M.A.; Speisky, H.; Lissi, E.; et al. Mechanism of pyrogallol red oxidation induced by free radicals and reactive oxidant species. A kinetic and spectroelectrochemistry study. *J. Phys. Chem. B* **2013**, *117*, 4870–4879. [CrossRef]
31. Dorfling, C.; Akdogan, G.; Bradshaw, S.M.; Eksteen, J.J. Modelling of an autoclave used for high pressure sulphuric acid/oxygen leaching of first stage leach residue. Part 1: Model development. *Miner. Eng.* **2013**, *53*, 220–227. [CrossRef]
32. Becci, A.; Amato, A.; Rodríguez Maroto, J.M.; Beolchini, F. Prediction model for Cu chemical leaching from printed circuit boards. *Ind. Eng. Chem. Res.* **2019**, *58*, 20585–20591. [CrossRef]

33. Faraji, F.; Alizadeh, A.; Rashchi, F.; Mostoufi, N. Kinetics of leaching: A review. *Rev. Chem. Eng.* **2022**, *38*, 113–148. [CrossRef]
34. Garcia, J.C.; Bareño, J.; Yan, J.; Chen, G.; Hauser, A.; Croy, J.R.; Iddir, H. Surface structure, morphology, and stability of Li($Ni_{1/3}Mn_{1/3}Co_{1/3}$)O_2 cathode material. *J. Phys. Chem. C* **2017**, *121*, 8290–8299. [CrossRef]
35. Billy, E.; Joulié, M.; Laucournet, R.; Boulineau, A.; De Vito, E.; Meyer, D. Dissolution mechanisms of $LiNi_{1/3}Mn_{1/3}Co_{1/3}O_2$ positive electrode material from lithium-ion batteries in acid solution. *ACS Appl. Mater. Interfaces* **2018**, *10*, 16424–16435. [CrossRef]

Disclaimer/Publisher's Note: The statements, opinions and data contained in all publications are solely those of the individual author(s) and contributor(s) and not of MDPI and/or the editor(s). MDPI and/or the editor(s) disclaim responsibility for any injury to people or property resulting from any ideas, methods, instructions or products referred to in the content.